Membrane and Water Treatment, *Vol. 10, No. 2 (2019) 165-178*
DOI: https://doi.org/10.12989/mwt.2019.10.2.165

PVA/H-β zeolite mixed matrix membranes for pervaporation dehydration of isopropanol-water mixtures

Zhen Huang*, Xiao-Fei Ru, Yu-Hua Guo, Ya-Tong Zhu and Li-Jun Teng

Department of Packaging Engineering, Institute of Materials Science & Chemical Engineering, Tianjin University of Commerce, Tianjin 300134, PR China

(Received September 28, 2018, Revised February 11, 2019, Accepted February 12, 2019)

Abstract. Mixed matrix membranes (MMMs) of poly (vinyl alcohol) (PVA) containing certain amounts of H-β zeolite for pervaporation were manufactured by using a solution casting protocol. These zeolite-embedded membranes were then characterized with scanning electron microscope (SEM), X-ray diffraction (XRD) and swelling tests. The membrane separation performance has been examined by means of isopropanol (IPA) dewatering from its highly concentrated aqueous solutions via response surface methodology (RSM). The results have demonstrated that the influences of feed IPA composition (85-95 wt.%), feed temperature (50-70°C), zeolite loading (15-25 wt.%) and their interactive influences are all statistically significant on both pervaporation flux (398-1228 g/m^2·h) and water/isopropanol separation factor (617-2001). The quadratic models based on the RSM analysis have performed excellently to correlate experimental data with very high determination coefficients and very low relative standard deviations. The optimal pervaporation predictions given by using the RSM models demonstrate a total flux of 953 g/m^2·h and separation factor of 1458, and are excellently verified by experimental results. As reflected by these results, PVA MMMs embedded with hydrophilic H-β zeolite entities have performed considerably better than its pure counterpart and indicated great potential for isopropanol dehydration applications.

Keywords: isopropanol dehydration; pervaporation; H-β zeolite; PVA; mixed matrix membrane

1. Introduction

Isopropyl alcohol or 2-propanol (*i.e.*, IPA) is a very important and extensively-used organic solvent in biopharmaceutical and chemical industries. Its applications and productions usually involve more or less amount of water in various liquid streams and thus it becomes necessary to purify IPA from its aqueous solutions. Unfortunately, a separation problem occurs because IPA and water form a minimum boiling azeotrope at IPA mass fraction of 87.4%, and the azeotropic temperature is 353.45 K at 101.3 kPa (Zhang *et al*. 2016, Devi *et al*. 2017). For the separation of such azeotropic mixture, the conventional distillation separation is usually inefficient and some other distillation techniques such as extractive distillation, pressure swing distillation, azeotropic distillation, or salt adding distillation may be a choice. For example, azeotropic distillation process has been frequently suggested for separating binary azeotropes in the literature (Devi *et al*. 2017) but an entrainer should be used, which has subsequently involved in the recovery of the entrainer used regardless any possible environmental problem. In contrast, the membrane-based pervaporation process is a promising, efficient, economic and eco-friendly separation method to separate the azeotropic liquid-liquid mixtures such as IPA-water. Thus, pervaporation has been considered as the most potential candidate for conventional distillation as highlighted in recent reviews (Bolto *et al*. 2011, Mahdi *et al.* 2015, Jia and Wu 2016, Ong *et al*. 2016, Wang *et al*. 2016).

In pervaporation, a liquid mixture is fed to a membrane on one side, some of the penetrant species are able to preferentially dissolve in and pass through the membrane, and finally evaporated and condensed from the other permeate side. The vapor pressure difference between the upstream feed mixture and the downstream permeate provides the driving force of the pervaporation process. As such, the permeate side is always kept under a vacuum, producing a pressure far below the saturated pressure of the penetrant species. The separation performances of a pervaporation membrane for a specific liquid mixture are usually evaluated in terms of permeate flux and separation factor, which is mainly related to the characteristics of the membrane materials. To promote the membrane separation properties, inorganic filler-incorporated mixed matrix membranes have recently been developed rapidly for pervaporation process, which have combined superior pervaporation separation preference of inorganic materials and excellent film-forming nature of organic polymers. A number of different inorganic fillers such as graphene oxide (Salehian and Chung 2017a, Salehian and Chung 2017b), metal oxide (Jiang *et al*. 2007, Dudek *et al*. 2014, Olukman and Sanli 2015, Dudek *et al*. 2017, Dudek *et al*. 2018), MOF (Wang *et al*. 2017), ZIF (Shi *et al*. 2012, Amirilargani and Sadatnia 2014, Ding *et al*. 2016, Hua *et al*. 2014, Wang *et al*. 2016), zeolite (Huang *et al*. 2006a, Huang *et al*. 2006b, Mosleh *et al*. 2012, Khosravi *et al*. 2012, Premakshi

*Corresponding author, Professor
E-mail: huangzhen50@yahoo.com

ISSN: 2005-8624 (Print), 2092-7037 (Online)

et al. 2015, Malekpour *et al*. 2017), silica (Das *et al*. 2011, Razavi *et al*. 2011, Choudhari *et al*. 2016) and carbon nanotubes (Shirazi *et al*. 2011, Amirilargani *et al*. 2013, Sajjan *et al*. 2013, Amirilargani *et al*. 2014) have been attempted in the fabrications of organic-inorganic mixed matrix membranes.

There are a lot of different kinds of pervaporation membranes for various application fields which are heavily dependent on the physicochemical characteristics of the membrane materials. For the dehydration of organics by means of pervaporation, hydrophilic polymer membranes are demanded as they can preferentially remove water from the feed solution while leaving the organic in the retentate. These hydrophilic polymers include poly (vinyl alcohol) (PVA) (Huang *et al*. 2006a, Huang *et al*. 2006b, Das *et al*. 2011, Razavi *et al*. 2011, Shirazi *et al*. 2011, Deng *et al*. 2016), chitosan (Kang *et al*. 2013, Premakshi *et al*. 2015, Fazlifard *et al*. 2017), cellulose (Dogan and Hilmioglu 2010, Zafar *et al*. 2012), alginate (Sajjan *et al*. 2013, Choudhari *et al*. 2016) and polyimide (Khosravi *et al*. 2012, Mosleh *et al*., 2012, Shi *et al*. 2012, Amirilargani *et al*. 2013, Amirilargani *et al*. 2014, Amirilargani and Sadatnia 2014, Hua *et al*. 2014, Salehian and Chung 2017a, Salehian and Chung 2017b). In our earlier works (Huang *et al*. 2006a, Huang *et al*. 2006b), highly hydrophilic PVA has been selected for ethanol dehydration due to the presence of many polar hydroxyl groups within its macromolecular chains that can strongly interact with water molecules. To this polymer, a number of zeolites have been incorporated to form a series of mixed matrix membranes and the experimental results have showed that the zeolite with higher hydrophilicity and smaller pore size seems to have resulted in much higher water/ethanol separation factor than those with lower hydrophilicity and a little larger pore size. For this reason, hydrophilic H-*β* zeolite was chosen as a modifier to PVA membranes to further our study on pervaporation dehydration of alcohols. It may be noted that H-*β* zeolite belongs to the BEA framework structure that possesses relatively intricate sinuous three-dimensional channel systems, and may discriminate competing molecules on a basis of the difference in molecular shape (Breck 1964).

In present study, the influences of zeolite loading, feed IPA composition and feed temperature on pervaporation dehydration for IPA/water mixture systems have been investigated systematically by using response surface methodology (RSM). It has been reported that the statistical RSM analysis is the most powerful mathematical tool to study the influences of multiple process variables on response parameters, and thus the number of experimental runs can be considerably reduced with high efficiency, resulting in a set of mathematical models for performing factor analysis (Ali and Hamrouni 2016, Chew *et al*. 2017, Choudhury and Ray 2017, Danmaliki *et al*. 2017, Vural *et al*. 2018). For example, Choudhury and Ray (2017) have carried out the investigation of ethanol dehydration through sodium montmorilonite-filled copolymer of acrylonitrile and acrylic acid, and the effect of copolymer composition, montmorilonite content and feed water concentration at a constant feed temperature of 30°C on the membrane pervaporation results are optimized by response surface methodology (RSM) using Box-Behnken design (BBD). Consequently, the significances of these factors and their interactive effects have been analyzed in detail for achieving the optimum membrane performance in terms of pervaporation flux and separation factor.

The aims of this work are 1) to cast a number of H-β zeolite/PVA mixed matrix membranes of different zeolite loadings and evaluate the MMM properties by means of SEM, XRD and swelling tests; 2) systematically examine the influences of zeolite loading, feed IPA composition and feed temperature, for the first time, on pervaporation results by using RSM analysis combined with Box-Behnken design (BBD). Based on the analysis results, a set of mathematical models have thus been developed for the permeate flux and water/IPA separation factor along with the optimum pervaporation conditions.

2. Experimental

2.1 Membrane preparations

The H-*β* zeolite-filled PVA MMMs and pure PVA membrane were fabricated via a solution casting method. Aqueous PVA solution having a concentration of 12 wt. % was made by adding 12.0 g of PVA (a 1750 degree of polymerization and 99% degree of hydrolysis, Tianjin Guangfu Fine Chemical Co., LTD, China), 1.0 g of fumaric acid (FA, 99.0%, Tianjin Guangfu Fine Chemical Co., LTD, China) and 88.0 g of double-distilled water into a 250 mL round bottom flask, followed by heating the flask under agitation in a water bath at 95°C for 12 h. Fumaric acid was employed as the cross-linking agent to PVA (Huang *et al*. 2006a, Huang *et al*. 2006b). For preparing zeolite/PVA dopes, the polymer sample was sequentially added into the flask to produce good zeolite-polymer contact and here 12.0 g of PVA was in three times added into the system for this purpose. The H-*β* zeolite was purchased from Tianjin Nankai Catalyst Co., LTD, China and it had a SiO_2/Al_2O_3 molar ratio of 38 and a particle dimension of about 1 μm. The zeolite powder of a designed amount was added into 88.0 g of distilled water under stirring for 1 h, followed by adding 4 g of PVA and 1.0 g of fumaric acid into the flask. The mixture was stirred and heated at 95°C for another 4 h. The left PVA was added twice into the above mixture and continuously stirred for 12 h to yield an apparently homogeneous dope. Before membrane casting, the dopes thus obtained were all statically placed in a fumehood for 12 h for removing bubbles. The casting was made onto a 30 cm×40 cm clean glass and flattened with a casting blade. After dried ambient in the fumehood for 24 h, the nascent films with or without zeolite were all heated at 160°C for 2 h for cross-linking purpose. All the membranes were kept in an air-tight dryer prior to any further measurements.

2.2 Characterizations of PVA-based MMMs

A scanning electron microscope (SEM, SS-550, Shimadzu) along with energy dispersive analysis (EDX) was attempted on various PVA-based MMM samples to

investigate the membrane morphologies. To obtain the MMM cross-sections, the sample strips were chilled in liquid nitrogen for a few minutes and then cracked with forceps to result in a sharply-broken cross-section for SEM analysis. A Rigaku D/max 2500v/PC X-ray diffraction (XRD) analyzer was employed to examine the crystalline structures of PVA/zeolite MMM samples and XRD measurements were scanned at a speed of 8°/min with a diffraction angle θ range of 2θ = 3-50°. The swelling measurements of all the MMMs were performed at 30°C gravimetrically in pure water and a binary IPA/water mixture having a water content of 90 wt. %. The dried membrane samples, after weighed on a digital microbalance (±0.01 mg, FA2104S, Shanghai Jingke Industrial Co. Ltd, China), were immersed in pure water and water-IPA mixture in sealed flasks at 30°C for 48 h. The swollen membranes were measured very quickly after carefully blotting the water residual from the sample surface. All the swelling measurements were repeated three times and the averaged data were taken. The percent degree of swelling (*DS*) was calculated as

$$DS(\%) = \frac{m_1 - m_0}{m_0} \times 100 \quad (1)$$

where m_1 and m_0 are the mass of the swollen and dried membrane samples, respectively.

2.3 Pervaporation experiments

The experimental setup used in this work is shown in Fig. 1 for pervaporation dehydration of isopropanol from its highly concentrated aqueous solutions, similar to the laboratory-scale Sulzer Chemtech pervaporation system used in our earlier works for ethanol dehydration (Huang *et al*. 2006a, Huang *et al*. 2006b). The experimental operating procedure may be described as follows. A circular testing film sheet after properly cut with a working area of 13.8 cm^2 was fixed into the stainless steel permeation cell. A series of aqueous IPA solutions of different concentrations were prepared with IPA (analytical grade, 99.7%, Tianjin Kaitong Chemical Reagent Co. Ltd., China) and double-distilled water. After adding 4.0 L IPA solution into the 5 L feed container, the resultant feed mixture was circulated via a pump at a flow rate of 40 L/h. The feed temperature was monitored to desired values with a circulating oil-heating close system while the downstream was maintained at around 100 Pa by applying a vacuum pump. The evaporated permeate was cold-trapped using liquid N_2 and collected in a round-bottom flask for mass measurement and composition analysis. It may be noted that steady permeation should be reached after varying feed temperature before collecting the penetrant sample for analysis.

The mass of collected samples and its IPA composition were measured using a digital balance (± 0.01 mg) and a gas chromatography analyzer (GC 1100 Beijing Purkinje General Instrument Co., Ltd.), respectively. The GC analysis was performed with a thermal conductivity detector and on an HP-5MS fused silica capillary column (30 m×0.25 mm i.d., 0.25 μm film thickness) with a

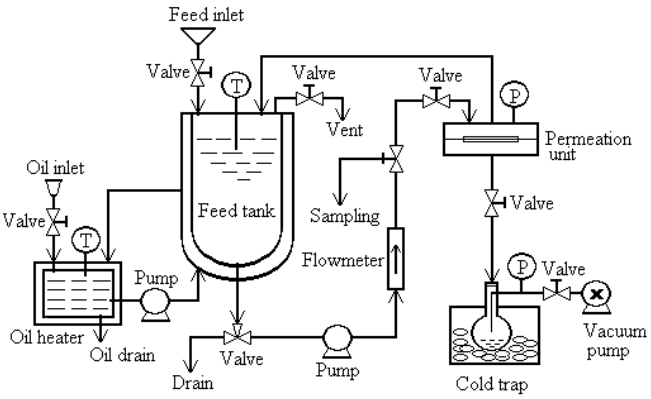

Fig. 1 A schematic of experimental pervaporation setup used in this study for IPA dehydration: T, temperature controller; P, pressure indicator

stationary phase of 5% pheny methyl-siloxane. The column temperature was initially 180°C and programmed to increase at a rate of 5°C/min to 200°C for 10 min and then at a rate of 10°C/min to 280°C for 5 min. The carrier gas used was Helium at a flow rate of 2.0 ml/min and the injection volume was 1 μL in a split mode. The injection and detector temperatures used were 210 and 250°C, respectively. For each pervaporation condition, measurements were independently carried out in triplicate and the values of flux and separation factor were thus averaged over measurements, leading to acceptable reproducibility with standard errors of <3%.

The pervaporation performances of H-β zeolite/PVA MMMs were evaluated in terms of total pervaporation flux (F) and water over IPA separation factor (α), and they were calculated using the following expressions

$$F_{total} = M / St \quad (2)$$

$$\alpha = \frac{y_{water} / y_{IPA}}{x_{water} / x_{IPA}} \quad (3)$$

where M (g) is the total mass of the collected permeate, t (h) is the time interval used for steady state permeation, S is the working area of 13.8 cm^2, x and y are the mass fraction of either water or IPA in the feed and permeate, respectively.

2.4 Experimental design and statistical analysis

In present study, a statistically factorial experimental method, Box-Behnken design (BBD) integrated with RSM analysis, was employed to examine the separation performances of H-β zeolite/PVA MMMs since this method generally allows investigators to study the influences of different variables considered by carrying out a relatively few experiments (Ali and Hamrouni 2016, Chew *et al*. 2017, Choudhury and Ray 2017, Danmaliki *et al*. 2017, Vural *et al*. 2018). According to a review paper (Smitha *et al*. 2004), feed composition and feed temperature are the most two important variables to affect the membrane performance. Sometimes the partial pressure difference across the membrane is also important but usually the

attention to it is to maintain the downstream side at a constant pressure value by applying vacuum. For zeolite-embedded MMMs, the zeolite loading is relatively critical to the membrane separation properties (Huang *et al*. 2006a, Huang *et al*. 2006b, Khosravi *et al*. 2012, Mosleh *et al*. 2012, Premakshi *et al*. 2015, Malekpour *et al*. 2017). As such, the zeolite loading, feed composition and feed temperature were taken as three independent variables and their influences on pervaporation performances of PVA-based MMM membranes were examined so that their significant levels for the RSM experiments could be determined.

In our earlier works (Huang *et al*. 2006a, Huang *et al*. 2006b), the effects of the above-mentioned factors on the membrane separation performances have been investigated by means of traditional one-variable-each-time method. According to the results thus achieved, the levels of the variables X_1 (feed temperature, °C), X_2 (feed IPA concentration, wt. %) and X_3 (zeolite loading, wt. %) have been chosen for the present RSM design. Table 1 lists the minimum, medium and maximum values of three independent variable which are coded to be −1, 0 and +1 levels, respectively. There are totally 17 runs for the three-variable, three-level BBD experimental design and the designed experiments were independently repeated three times and averaged values were used for subsequent analyses. For performing RSM analysis for our three variable-three level case, a polynomial quadratic model can be suggested

$$R = b_0 + \sum_{i=1}^{N} b_i X_i + \sum_{i=1}^{N} b_{ii} X_i^2 + \sum_{i=1}^{N} \sum_{j\geq 2}^{N} b_{ij} X_i X_j \qquad (4)$$

where R is the response, X_i and X_j are the independent variables involved, b_0 is a constant coefficient, b_i, b_{ii}, and b_{ij} are the regression coefficients of linear, quadratic and interaction terms, respectively, and N is the number of the variables considered. The values of three variables (zeolite loading, feed temperature and feed IPA concentration) were then determined with the polynomial quadratic model for achieving maximum permeation flux or maximum separation factor.

The fit of the regressed polynomial model against experimental data and then finding the optimal process conditions were performed by using the Design- Expert software version 7.1.3. By means of analysis of variance (ANOVA) of the data thus obtained, the goodness of fit of the regression model was evaluated by considering the determination coefficient (R^2), the adjusted determination coefficient (R_a^2) and the relative standard deviation (*RSD*). The former two coefficients are used to analyze the model accuracy, representing the proportion of the total variations that could be covered by the fitted model. The RSD defined as a ratio of the standard deviation to the mean value of observed response is used to express the precision and repeatability of the regressed model. The statistical significance of the independent variables and their interactions was analyzed with F-test to obtain the mathematical relationship between input and output parameters and it can be thought significant if the obtained P-value is <0.05. The ranges of the independent variables for leading to desirable results might be visually determined by analyzing three-dimensional response surface plots of the independent and dependent variables.

Table 1 Independent variables and their levels used in the RSM design

Symbol	Variables	Coded variable level		
		minimum	medium	maximum
		-1	0	1
X_1	Feed temperature (°C)	50	60	70
X_2	Feed IPA concentration (wt. %)	85	90	95
X_3	Zeolite loadings (wt. %)	15	20	25

3. Results and discussion

3.1 Characterizations of PVA/zeolite MMMs

3.1.1 SEM result

The surface and cross-sectional morphologies of the zeolite-embedded PVA membranes were evaluated by means of SEM to study how about the compatibility achieved between the inorganic zeolite and organic PVA matrix. Fig. 2 shows SEM images of the PVA membranes with and without an H-β zeolite loading of 20 wt. %. As can be seen from Fig. 2(a), the unfilled PVA membrane shows very smooth surface and its cross-sectional surface also looks smooth but with some small particles as shown in Fig. 2(b), possibly due to the forceps-folding preparation in liquid nitrogen. As to the MMM of 20 wt. % H-β zeolite loading, it can be seen from Fig. 2(c) that the membrane surface is relatively well-distributed with zeolite particles. The membrane looks apparently dense and defect-free if observing the cross-sectional SEM image in Fig. 2(d). Furthermore, the zeolite particles seem to embed with PVA matrix tightly and no observable defects like pores or cavities can be observed in the membrane for 20 wt. % loading. The SEM results shown in Figs. 2(c) and 2(d) suggest very good inorganic-organic contact between the dispersed filler phase and continuous matrix phase. The EDX analysis has resulted in an atomic percentage of 95.2 and 4.8 for Si and Al, respectively. Then it can be deduced that the Si/Al molar ratio is 19.83 or equivalent to a SiO_2/Al_2O_3 molar ratio of 39.7, close very well to the SiO_2/Al_2O_3 molar ratio of 38 released by the production company.

3.1.2 XRD result

Fig. 3 shows the XRD analysis results for the 20 wt. % H-β zeolite filled MMM, unfilled PVA membrane and H-β zeolite powder. It can be observed that the unfilled PVA membrane exhibits a very broad peak of around 2θ = 20°, which is typical of not fully complete crystallization for semi-crystalline polymers. This peak still retains very well after crosslinked with a small amount of formic acid, indicative of relatively appreciated degree of crystallinity.

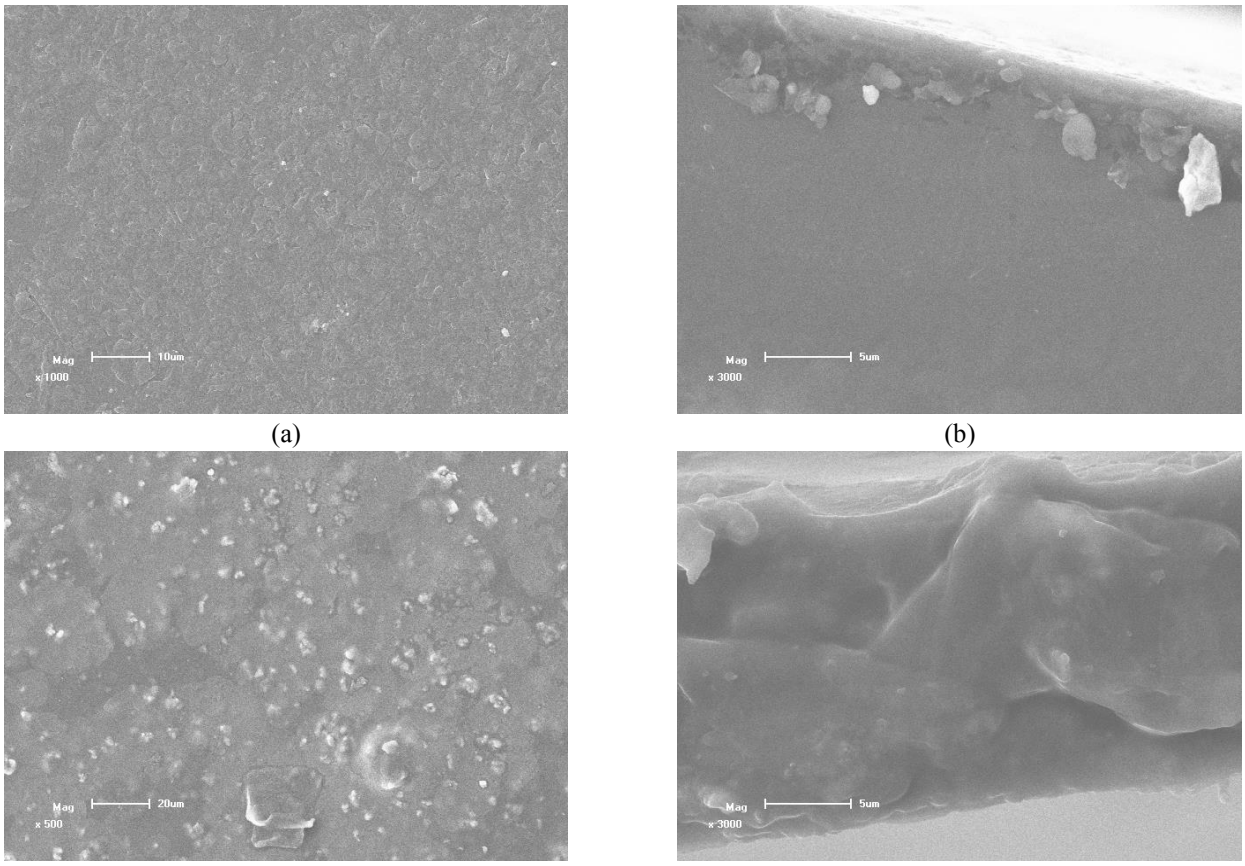

Fig. 2 SEM images of the PVA based membranes without (a) & (b) and with (c) & (d) an H-*β* zeolite loading of 20 wt. %: a & (c) top view; (c) & (d) cross-sectional view

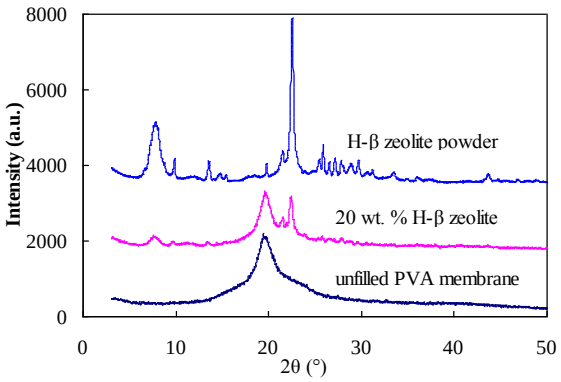

Fig. 3 XRD results of H-*β* zeolite powder, unfilled PVA and filled MMM samples

For the 20 wt. % zeolite-loaded MMM sample, XRD pattern shows that the intensity of the characteristic peak at $2\theta = 20°$ drops significantly when compared to that of the unfilled PVA membrane, suggesting that the presence of H-*β* zeolite in the membrane matrix has consequently led to the substantial decrease in the relative crystallinity of the parent polymer PVA. Besides, some other peaks are seen to be at about $2\theta = 8°$, 9° and 23° for the MMM sample, and these peaks could be attributed to the H-*β* zeolite incorporated into the MMM if looking through XRD patterns of H-*β* zeolite powder given in Fig. 3 as well.

3.1.3 Swelling result

Fig. 4 presents the swelling measurements of H-*β* zeolite/PVA MMMs of different zeolite loadings tested in pure water and water/IPA mixture with water content of 90 wt. %. For pervaporation applications, the swelling behaviour of polymer-based membranes generally represents the capability of forming specific interactions between polymer macromolecules and the absorbed molecules and thereafter dominates the forward transport of dissolved molecules through the membrane. It can be seen from Fig. 4 that the PVA membrane without zeolite particles can swell very well in pure water and the degree of swelling reached is 57.4% even after it has been crosslinked with fumaric acid. The reason for it can be explained as the main contribution of hydrogen-bonding interactions formed between the hydroxyl groups of PVA macromolecules and water molecules. Once changing pure water to IPA/water mixture, the PVA membrane shows decreased DS value, which in turn indicates that the membrane exhibits higher preference to water than to IPA and the presence of IPA seems to compress the membrane swelling. Such result is understandable since water is more polar than IPA, and forms relatively stronger interaction than IPA with the hydroxyl groups of PVA molecules, consequently leading to more pronounced membrane swelling. For the H-*β* zeolite filled PVA membranes, they show compressed swelling behavior in either pure water or water/IPA solution as

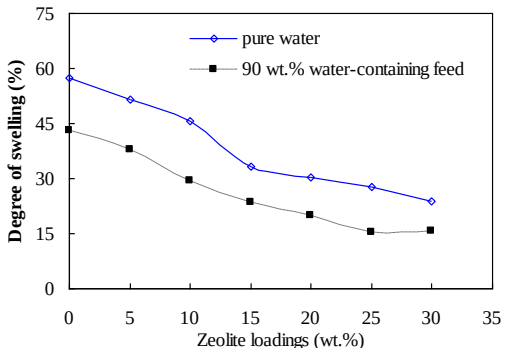

Fig. 4 Swelling results of PVA-based MMMs of different H-β zeolite loadings in pure water and 90 wt. % water-containing IPA mixture

compared to pure PVA counterpart and the DS value of the MMMs is clearly seen to decrease with the increase in the zeolite loading. That is to say that the unfilled PVA membrane has possessed the highest DS value in either water or its IPA mixture.

The compressed swelling of the PVA-based MMMs may be due to that: 1) The free volume of PVA membrane has experienced a great reduction because of the incorporation of zeolite entities in polymer matrix, subsequently leading to the drop of water swelling. The micro-sized zeolite powders may occupy the free volume formed among macromolecules to certain extent. In the meantime, the H-β zeolite particles embedded still retain its framework rigidity because of its crystalline structure (please refer to Fig. 3) and may behave as the physical crosslink points in the PVA matrix (Amnuaypanich *et al.* 2009, Khoonsap and Amnuaypanich 2011), and then restrict the flexible movement of PVA chains surrounding the rigid zeolite particles to yield new free volume. 2) The mass of PVA in the MMM samples is monotonously decreased as the zeolite loading increases whereas the H-β zeolite incorporated into the PVA matrix possesses rather poorer water absorption capability than the PVA parent counterpart. In other word, the compensation to less water swelling arising from the reduced PVA mass cannot be made up by introducing the same mass of hydrophilic H-β zeolite, reflecting the ability of zeolite to suppress the PVA membrane swelling.

3.2 Response surface analysis of experimental results

3.2.1 Fitting the model against the experimental data

Taking feed temperature (°C, X_1), feed IPA concentration (wt. %, X_2) and zeolite loadings (wt. %, X_3) as three independent variables, the RSM analysis coupled with experimental BBD design has been adopted by considering total pervaporation flux (g/m^2·h, Y_1) and water/IPA separation factor (Y_2) as two responses. The experimental data obtained from the seventeen-run experiments are given in Table 2. It can be seen that total flux and separation factor obtained with the filled PVA membranes are in the ranges of 398-1228 g/m^2·h and 617-2001, respectively, with different combinations of the independent variables. As a comparison, the unfilled PVA membrane has resulted in a dehydration separation factor of 328 and total flux of 424.54 g/m^2·h under 60°C and 80 wt. % IPA aqueous solution. Clearly, the PVA-based MMMs all demonstrate much better separation performance than the unfilled PVA membrane and result in higher separation factor values as shown in Table 2, indicating that the incorporation of H-β zeolite is undoubtedly favourable for the dehydration separation from highly concentrated IPA aqueous solution.

Table 2 Box-Behnken design of independent variables and experimental result

Run No.	X_1	X_2	X_3	Total flux(g/m^2·h)	Separation factor
1	-1	0	1	978.12±14.23	1405±6
2	0	0	0	677.11±11.45	1626±9
3	1	-1	0	1094.88±15.54	856±7
4	-1	1	0	397.89±12.09	2001±8
5	1	1	0	829.31±11.98	1563±7
6	0	-1	1	1163.4±13.33	795±7
7	0	0	0	684.48± 9.64	1638±6
8	0	1	-1	534.18±10.67	1256±8
9	0	-1	-1	709.43± 9.08	617±9
10	-1	0	-1	519.13±13.07	999±5
11	0	0	0	695.32±12.77	1610±4
12	-1	-1	0	785.66± 9.45	1318±8
13	0	1	1	794.18± 9.84	1456±3
14	1	0	-1	1038.12±11.12	751±10
15	0	0	0	676.56± 8.96	1614±3
16	0	0	0	699.34±10.97	1599±7
17	1	0	1	1228.32±10.32	854±5

In this work, the two responses are equally considered in the RSM method, and then the experimental data for both responses are statistically analyzed in parallel through the variance analysis of the variables investigated. The mathematical model generated from experimental data has been obtained by means of Design-Expert 7.1.3 software program, and the P-value, resulting from the RSM analysis, is then used to evaluate the statistical significance of all model coefficients regressed.

Based on the measurement results given in Table 2, the predicted value Y_1, for total pervaporation flux, has been fitted into the polynomial equation with a multiple regression procedure and the results of the RSM analysis are presented in Table 3. The RSM quadratic model obtained for total pervaporation flux can be expressed as follows

$$\begin{aligned} Y_1 = {} & 686.56 + 188.73X_1 - 149.73X_2 + 170.40X_3 \\ & + 30.55X_1X_2 - 67.20X_1X_3 - 48.59X_2X_3 \\ & + 115.50X_1^2 - 25.13X_2^2 + 138.86X_3^2 \end{aligned} \quad (5)$$

where Y_1 is the total pervaporation flux (g/m^2·h), X_1 is the feed temperature (°C), X_2 is the feed IPA concentration (wt. %) and X_3 is the zeolite loading (wt. %).

To evaluate whether the fitted model is good or not, the coefficient of determination (R^2) and the statistical

Table 3 Analysis of variance results for response surface quadratic model of total pervaporation flux

Source of variation	Degree of freedom	Sum of squares	Mean squares	F-value	P-value	Significance*
Model	9	8.73×10^5	9.70×10^4	2.67×10^2	< 0.0001	significant
X_1	1	2.85×10^5	2.85×10^5	7.85×10^2	< 0.0001	significant
X_2	1	1.79×10^5	1.79×10^5	4.94×10^2	< 0.0001	significant
X_3	1	2.32×10^5	2.32×10^5	6.40×10^2	< 0.0001	significant
X_1X_2	1	3.73×10^3	3.73×10^3	10.3	0.0149	significant
X_1X_3	1	1.81×10^4	1.81×10^4	49.7	0.0002	significant
X_2X_3	1	9.41×10^3	9.41×10^3	25.9	0.0014	significant
X_1^2	1	5.62×10^4	5.62×10^4	1.55×10^2	< 0.0001	significant
X_2^2	1	2.66×10^3	2.66×10^3	7.32	0.0304	significant
X_3^2	1	8.12×10^4	8.12×10^4	2.24×10^2	< 0.0001	significant
Residual	7	2.54×10^3	3.63×10^2			
Lack of fit	3	2.11×10^3	7.03×10^2	6.48	0.0514	insignificant
Pure error	4	4.32×10^2	1.08×10^2			
Corrected total	16	8.76×10^5				
RSD = 2.35 %		R^2 = 0.9971		R_a^2= 0.9926		

*significant at P < 0.05.

significance of the regressed model are examined with the F-test to mathematically correlate the input with output parameters (Chew *et al*. 2017, Danmaliki *et al*. 2017). The results thus obtained are included in Table 3 along with the statistical significance analysis results summarized for all regression coefficients. It is seen from Table 3 that the F-test value and P-value for the quadratic model are 267.19 and 0.0001 (<0.001), respectively, suggesting that the model regressed according to the RSM method is of great statistical significance. The determination coefficient (R^2) thus obtained is 0.9971, indicative of an excellent fit of the model against the experimental data. The accuracy of the fitted model has been further validated by the adjusted determination coefficient (R_a^2) of 0.9926 and a non-significant lack of fit with a P-value of 0.0514 (>0.05). In the meantime, the regression model may have resulted in very satisfactory reproducibility as confirmed by the very low value of the relative standard deviation (RSD = 2.35%).

It can be seen from Table 3 that, the influences of three independent variables (feed temperature, feed IPA concentration and zeolite loading) on the total pervaporation flux are all statistically significant as reflected by the P-values (P< 0.001) of the regressed coefficients of the model linear terms (X_1, X_2 and X_3), all quadratic terms (X_{12}, X_{22} and X_{32}), and all interaction terms (X_1X_2, X_1X_3 and X_2X_3). Feed temperature and zeolite loading are both seen from Eq. (5) to demonstrate positive influences and their positive changes will lead to a significant increase in the pervaporation flux. That is to say, the total flux is increasing as either feed temperature or zeolite loading increases. This appears to be understandable and can be explained as follows. In the case of higher feed temperature, the polymer matrix becomes structurally looser, rendering polymer free volume become larger for the penetrate species to transport through more easily. In the meantime, the permeating molecules become more active and more readily to move forward at higher feed temperature. As such, the pervaporation flux tends to rise as feed temperature increases. On the other hand, the increasing dependence of pervaporation flux on the zeolite loading is closely related to the properties of H-*β* zeolite used, i.e., hydrophilic characteristic and large pore dimension. The hydrophilic feature, as reflected by the presence of appreciable amounts of the Al atoms in the zeolite framework (Breck 1964), could have rendered zeolite entities form strong interactions with water molecules, thus promoting water easily transporting across the mixed matrix membranes. Porous H-*β* zeolite is reported to possess a channeling system with a pore aperture of 0.71 nm×0.73 nm or 0.56 nm×0.57 nm (Breck 1964), which is much larger than the kinetic diameter of either water molecule (0.296 nm) or IPA molecule (0.470 nm) (Wang *et al*. 2009), rendering two species relatively readily go through the MMM by taking full advantage of zeolitic channeling system and thus resulting in higher flux at higher zeolite loading.

However, the IPA concentration in the feed mixture, based on Eq. (5), has a negative influence on the pervaporation flux and the increase in the feed IPA content results in a considerable decrease in pervaporation flux. This finding could be attributed to the coupling function happening between water and IPA molecules. It is known that both H-*β* zeolite filler and PVA polymer matrix are of hydrophilic feature, and water molecules possess higher polarity than IPA molecules. Due to the coupling function (Huang *et al*. 2006b), the IPA species could drag the forward transport of water molecules whereas the water species could pull the forward movement of the IPA molecules. At higher feed IPA content, the coupling function seems to be more considerable for the slow IPA and the mutual effect between IPA and water molecules has subsequently led to lower IPA permeation and lower water

Table 4 Analysis of variance results for response surface quadratic model of separation factor

Source of variation	Degree of freedom	Sum of squares	Mean squares	F-value	P-value	Significance*
Model	9	1.57×10^6	1.74×10^4	3.77×10^2	< 0.0001	significant
X_1	1	3.61×10^5	3.61×10^5	4.70×10^2	< 0.0001	significant
X_2	1	9.04×10^5	9.04×10^5	1.18×10^3	< 0.0001	significant
X_3	1	9.84×10^4	9.84×10^4	1.28×10^2	< 0.0001	significant
X_1X_2	1	1.41×10^2	1.41×10^2	0.18	0.681	insignificant
X_1X_3	1	2.31×10^4	2.31×10^4	30.2	0.0009	significant
X_2X_3	1	1.20×10^2	1.20×10^2	0.16	0.7042	insignificant
X_1^2	1	4.73×10^4	4.73×10^4	61.6	0.0001	significant
X_2^2	1	2.49×10^4	2.49×10^4	32.4	0.0007	significant
X_3^2	1	1.09×10^5	1.09×10^5	1.42×10^3	< 0.0001	significant
Residual	7	5.37×10^3	7.67×10^2			
Lack of fit	3	4.45×10^3	1.48×10^3	6.43	0.052	insignificant
Pure error	4	9.23×10^2	2.31×10^2			
Corrected total	16	1.57×10^6				
RSD = 1.64 %		R^2 = 0.9979			R_a^2= 0.9937	

*significant at P < 0.05.

permeation as well. In other words, lower feed IPA concentration or higher water feed content can lead to higher pervaporation flux.

Apart from statistically significant influences of the linear terms as discussed above, all the quadratic terms are found to have a P-value considerably lower than 0.05, indicating that three variables have substantial second-order influence on the total pervaporation flux according to Eq. (5). Besides, all the interaction terms are also found of significance, indicating that the interactional influences of feed temperature and zeolite loading, feed IPA content and zeolite loading, and feed temperature and feed IPA content on total pervaporation flux are all significant, suggesting the presence of significant interacting effects among three independent variables.

In the case of water/IPA separation factor, another quadratic model has been generated by nonlinearly regressing against the experimental data, and the analysis results are summarized in Table 4. The second-order polynomial model may be represented as the following for water/IPA separation factor.

$$\begin{aligned} Y_2 = {} & 1617.43 - 212.38X_1 + 336.16X_2 + 110.90X_3 \\ & + 5.94X_1X_2 - 76.06X_1X_3 + 5.48X_2X_3 \\ & - 105.99X_1^2 - 76.89X_2^2 - 509.24X_3^2 \end{aligned} \quad (6)$$

As seen from Table 4, the F-value and P-value for the regressed model are 377.18 and <0.0001, respectively, seemingly suggesting that the quadratic model thus regressed is statistically significant. The model seems to be well-performed to correlate the experimental data and leads to a very satisfactory fit, as indicated by extremely high determination coefficient R^2 of 0.9979 and very high adjusted determination coefficient R_a^2 of 0.9937 as well (Chew *et al*. 2017, Danmaliki *et al*. 2017). Moreover, a non-significant lack of fit, with a P-value of 0.052, further suggests the model is workable for predicting water/IPA separation factor. At the same time, the *RSD* value thus obtained has a value of 1.64%, indicating that the model may lead to a high degree of precision and repeatability.

Like to that for total pervaporation flux, the influences of feed temperature, feed IPA concentration and zeolite loading on water/IPA separation factor are all greatly statistically significant as shown by the P-value of <0.001 for three model linear terms. It can be deduced from Eq. (6) that, feed IPA concentration and zeolite loading will have positive influences whereas feed temperature does negative influence on water/IPA separation factor. In other words, the increment of either feed IPA concentration or zeolite loading will lead to the increase in water/IPA separation factor while the increase of feed temperature tends to result in the decrease in water/IPA separation factor. Apparently, these observations are consistent very well with those reported in our earlier works for ethanol dehydration (Huang *et al*. 2006a, Huang *et al*. 2006b). The improved separation factor from feed IPA concentration may be due to the formation of relatively stronger interactions between hydrophilic membrane materials and more polar water molecules rather than less polar IPA molecules, consequently leading to more favorable transport of water molecules through the membrane. When more water molecules diffusing in the membranes, the coupling effect may take a role and the mutual dragging effect between IPA and water molecules leads to relatively higher IPA flux and then renders the hydrophilic membranes become less selective, resulting in decreased separation factor at higher feed water concentrations. As for the zeolite loading, the increased separation performance is probably attributed to the hydrophilic nature of H-β zeolite and its shape-selective sinusoidal channeling feature (Huang *et al*. 2006a). Actually, the MMM with a zeolite loading of 20 wt.% has demonstrated the highest separation factor, as discussed in

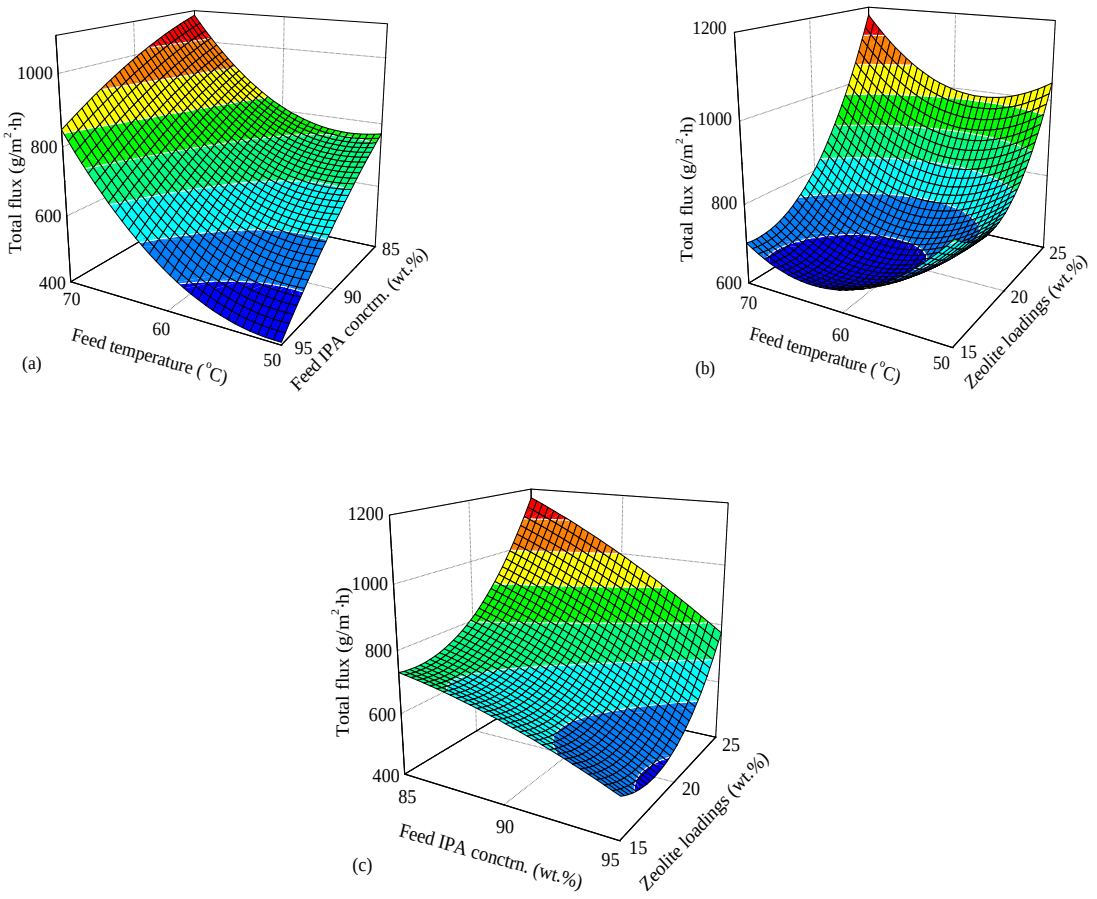

Fig. 5 Response surface plots showing the dependence of total pervaporation flux on (a) feed temperature and feed IPA concentration, (b) zeolite loading and feed temperature, (c) zeolite loading and feed IPA concentration

the following section. In the case of the negative temperature effect on separation factor, it may be due to that 1) the membrane microstructure becomes much looser at higher feed temperature, and thus less selective for two permeating molecules to go through, 2) two competing species are becoming volatile with feed temperature but IPA is more volatile.

According to Eq. (6), the quadratic terms of feed temperature and zeolite loading and their interaction term are all significant with a P-value of smaller than 0.001, and in the meanwhile their influences on water/IPA separation factor are all negative. The statistical significance of the model terms of feed temperature and zeolite loading indicates that the influence of feed temperature or zeolite loading on water/IPA separation factor is not a simple linear relationship but a rather complex one. In other words, both feed temperature and zeolite loading have significant first order linear influence and significant second-order influence on water/IPA separation factor. As for the feed IPA concentration, its quadratic term has a P-value of < 0.001 and thus is significant but its interaction terms (X_1X_2, X_2X_3) have resulted in a P-value higher than 0.05 and thus both are insignificant. Hence, feed IPA concentration tends to have significant first order linear influence and significant second-order quadratic influence on water/IPA separation factor. The quadratic regression model for water/IPA separation factor can be further revised once the non-significant terms are removed, resulting in a very simple model as given below

$$Y_2 = 1617.43 - 212.38X_1 + 336.16X_2 + 110.90X_3 - 76.06X_1X_3 - 105.99X_1^2 - 76.89X_2^2 - 509.24X_3^2 \quad (6a)$$

3.2.2 Response surface 3D plots

The RSM quadratic models obtained for pervaporation flux and separation factor are employed to research the influences of independent variables, i.e., feed temperature, feed IPA concentration and H-*β* zeolite loading, and their interactions on dependent responses of Y_1 (total pervaporation flux) and response Y_2 (separation factor). In order to visualize these influences, the 3D response surface graphs are plotted by sketching the response (*z*-axis) versus two independent parameters (*x* and *y* coordinates) varied in the experimental ranges while maintaining the other parameter constant at the zero-level. The zero values set for BBD experiments are 60°C, 90 wt. % and 20 wt. % for feed temperature, feed IPA concentration and H-*β* zeolite loading, respectively.

Fig. 5 visually presents the simultaneous influences of feed IPA concentration and H-*β* zeolite loading, feed

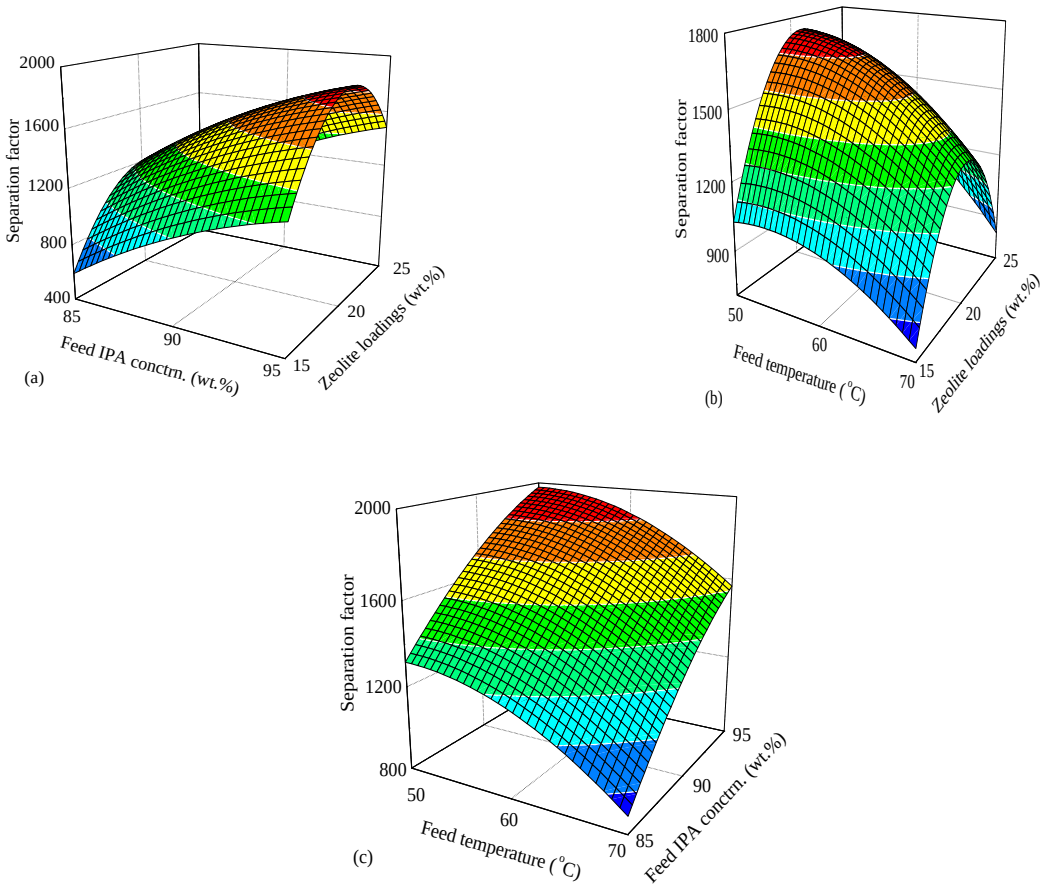

Fig. 6 Response surface plots showing the dependence of water/IPA separation factor on (a) zeolite loading and feed IPA concentration, (b) zeolite loading and feed temperature, (c) feed temperature and feed IPA concentration

temperature and H-β zeolite loading, and feed temperature and feed IPA concentration on total pervaporation flux, respectively. According to the 3D total flux plot, it can be seen that there does exist a desirable location in the design space as referred to red area in Fig. 5 where the response Y_1 of total pervaporation flux tends to have the highest value.

It can be seen from Fig. 5a that the total flux considerably increases with the decrease of the feed IPA concentration under different feed temperatures, while keeping the zeolite loading at constant. In the meanwhile, the total flux increases significantly with the increase of feed temperature under different feed IPA concentrations. Satisfactory larger pervaporation flux values may be obtained at around 70°C and a feed of 85 wt. % IPA aqueous solutions. Higher feed IPA concentration or lower feed temperature generally leads to the decrease of the overall pervaporation flux. It may be noted that the interaction influence of feed IPA concentration and temperature on the total flux is significant as the P-value is less than 0.05.

As seen from Fig. 5(b), the dependence of the overall flux on zeolite loading and feed temperature considered is not simple when feed IPA concentration is fixed at 90 wt. %. This might be due to their very significant interaction influence on the flux as reflected by the P-value (0.0002) far less than 0.05. When the zeolite loading is not higher than 20 wt. %, the total flux is less than 800 g/m^2·h as can be referred to blue and dark blue area in Fig. 5(b) regardless of the feed temperature considered. However, it can be seen that relatively larger flux values may be achieved at 70°C and 25 wt. % of zeolite loading. Fig. 5(c) shows that when keeping feed temperature at constant, the total flux generally increases with the increment of the zeolite loading but it considerably decreases as the feed IPA concentration goes up. At the same time, their interaction influence is noted to be significant ($P < 0.05$). Relatively larger flux values can be reached in the case of 85 wt. % IPA aqueous solution and 25 wt. % of zeolite loading.

Based on the 3D plots given in Fig. 6, it can be conveniently observed how the three independent factors to influence response two Y_2 (separation factor) and visually found as well the desirable response Y_2 in the 3D surface as coloured in red, similar to the case of the response one Y_1 (total flux). It can be seen from Fig. 6(c) that when the zeolite loading is kept constant, water/IPA separation factor considerably increases with the increase of the feed IPA concentration under different feed temperatures whereas it gradually decreases with the increase of the feed temperature irrespective of the feed IPA concentration used. Lower feed temperature and higher feed IPA concentration, as expected, can result in larger response value, i.e., higher separation factor, or vice versa. Relatively higher separation

Table 5 Comparison of IPA dehydration performances of recently reported pervaporation MMMs

Polymer	Filler	Feed IPA conc. (wt%)	Feed Temp.(°C)	Separation factor (α)	Flux (kg/m^2·h)	PSI (kg/m^2·h)	Ref.
6FDA-Durene/DABA (7:3)	NH_3-graphene oxide (0.5 wt %)	85	60	624	1.914	1192.42	Salehian and Chung (2017a)
P84	NH_3-graphene oxide (0.5 wt %)	85	60	6726	0.1615	1086.09	Salehian and Chung (2017b)
Sodium alginate	TEOS (30 wt %)	90	50	3741	0.1864	697.14	Choudhari *et al*. (2016)
chitosan	Zeolite NaY (40 wt %)	90	50	683	0.0126	8.59	Premakshi *et al*. (2015)
PVA	ZIF-8(5 wt %)	90	30	132	0.868	113.71	Amirilargani and Sadatnia (2014)
PVA	MWNTs-PSS (3 wt %)	90	50	220	0.225	49.28	Amirilargani *et al*. (2014)
P84	ZIF-90(30 wt %)	85	60	385	0.114	43.78	Hua *et al*. (2014)
P84	ZIF-90-SPES (30 wt %)	85	60	5668	0.109	617.71	Hua *et al*. (2014)
PVA	MWNT–PAH (1wt%)	90	30	948	0.207	196.03	Amirilargani *et al*. (2013)
Sodium alginate	CS wrapped MWCNTs (2 wt %)	90	50	2134	0.284	605.77	Sajjan *et al*. (2013)
Matrimid 5218	Zeolite 4A (15wt %)	90	50	3500	0.038	132.96	Khosravi *et al*. (2012)
Matrimid 5218	ZSM-5 (Si/Al=40, 10 wt %)	90	50	2100	0.025	52.48	Mosleh *et al*. (2012)
PBI	ZIF-8 (33.7 wt %)	85	60	1686	0.103	173.56	Shi *et al*. (2012)
PVA	Aluminosilicate (6 wt %)	87.7	50	46	0.12	5.40	Das *et al*. (2011)
PVA	APTEOS/TEOS (50wt %)	90	50	110	0.62	67.58	Razavi *et al*. (2011)
PVA	CNTs (2 wt %)	90	30	1794	0.079	141.65	Shirazi *et al*. (2011)
PVA	H-β zeolite (20 wt %)	90	60	1645	0.648	1065.31	This work
PVA	H-β zeolite (25 wt %)	85	50	1458	0.953	1389.47	This work

factor can be realized when feed temperature reaches 50°C and IPA concentration in the feed is about 95 wt. %. However, their interaction influence on separation factor is not significant as the P-value is lager than 0.05. Fig. 6(a) and 6(b) show that the separation factor increases first and then decreases with the increase of zeolite loading under different feed temperatures or different feed IPA concentrations. Regardless of the zeolite loadings investigated the water/IPA separation factor is seen to considerably decrease with the increase of feed temperature (Fig. 6(b)) or increase monotonously with the increase of feed IPA concentration (Fig. 6(a)). Relatively larger response value, namely the higher separation factor, can be obtained at around the H-β zeolite loading of 20 wt. %.

3.2.3 Experimental verification of model predictions

Based on the results given in Tables 3 and 4, feed temperature, feed IPA concentration and zeolite loading are all seen to significantly affect total pervaporation flux or water/IPA separation factor. Using the RMS quadratic model, the optimum variable levels can be mathematically figured out according to the Lagrange theory to make two responses achieve highly desirable values, and a set of optimum conditions thus obtained are 50.2°C of feed temperature, 89.8 wt. % of feed IPA concentration and 24.7 wt. % of H-β zeolite loading. These values were slightly adjusted for actual application purpose and they were 50°C, 90 wt. % and 25 wt. % for feed temperature, feed IPA concentration and H-β zeolite loading, respectively. Under such optimized conditions, the total pervaporation flux and water/IPA separation factor are predicted to be 953 g/m^2·h and 1458, respectively.

In order to assess the acceptability of the model prediction, the pervaporation test was carried out under optimized conditions. Three parallel experiments were conducted and the total pervaporation flux and separation factor thus determined and averaged were, respectively, 953 ± 10 g/m^2·h and 1458±8, which are in very good agreement with the predicted values given above. The deviations of predicted results from the experimental data are far less than ± 1.0%. Therefore, the optimum conditions determined by RSM have thus been verified, confirming that by means of RSM analysis the pervaporation dehydration of highly concentrated IPA aqueous solution can be reliably optimized for new PVA/H-β zeolite mixed matrix membranes.

3.3 Comparison with literature contributions

A comparison of the IPA dehydration performances of pervaporation MMMs recently published in the literatures and the PVA/H-β zeolite MMM is given in Table 5. Herein,

separation factors and total pervaporation fluxes along with operational conditions are all included and it can be seen that the newly developed MMM with 20 wt% H-β zeolite exhibits a comparable separation factor of 1645 for dehydrating 90 wt % IPA aqueous solution at 60°C and in the meantime it also possesses a very much higher pervaporation flux of 0.648 kg/m^2·h than most of other MMMs. Furthermore, one may see from Table 6 that the MMM newly-developed in our work has demonstrated superior dehydration separation performance in terms of Pervaporation Separation Index (PSI, i.e., PSI = F·(α-1)) if compared to the other MMMs. Based on such excellent pervaporation results, we may think that the PVA/H-β zeolite MMMs developed here can be greatly useful for potential alcohol pervaporation dehydrations.

4. Conclusions

In this study, we have investigated the influence of embedded H-β zeolite on the pervaporation separation of the PVA membranes for dewatering isopropanol aqueous solution. The PVA/H-β zeolite mixed matrix membranes were fabricated by using a solution casting method. The membrane pervaporation performances have been mainly evaluated in terms of the total flux and separation factor. The following conclusions may be drawn from present work:

• SEM images reflect that there appears to be very good contact between the dispersed H-β zeolite filler and continuous PVA matrix while XRD pattern indicates that the two phases have still retained their respective crystalline features even subjected to the presence of the other phase.

• Swelling results show that the zeolite addition has considerably compressed the PVA membrane swelling in water or IPA/water liquids, due to the inorganic nature and rather low water sorption capacity of H-β zeolite. The presence of IPA in the swelling test liquid has also compressed the membrane swelling because of the less polar property of IPA than water.

• Pervaporation results show the addition of H-β zeolite has varied the intrinsic properties of the PVA membrane via its hydrophilic feature and porous structure, and thus substantially increased the membrane water/IPA separation factor and pervaporation flux.

• The PVA-based MMMs shows higher separation factor when subjected to either higher feed IPA concentration or lower feed temperature, and the membrane tends to exhibit higher pervaporation flux when subjected to either higher feed temperature or lower feed IPA concentration.

• The RSM analysis coupled with a three-variable-three-level Box-Behnken Design was successfully employed to investigate the pervaporation performance of PVA/zeolite MMM for dewatering IPA aqueous solution. The quadratic models and 3D plots for total flux and separation factor have thus been established. The RMS quadratic models can fit very well against the experimental data, as confirmed by the very high R^2 values and rather low *RSD* values. The graphical 3D plots have visually described the interactive influences of zeolite loading, feed composition and feed temperature on the total flux and separation factor.

• The RSM analysis results demonstrate that all three variables are significantly influential for both total pervaporation flux and water/IPA separation factor and their interactive influences are also significant as well.

• Within the range considered, pervaporation conditions are optimized to be 50°C of feed temperature, 85 wt. % of feed IPA concentration and 25 wt. % of H-β zeolite loading. Under these conditions, the predictions are 953 g/m^2·h for total flux and 1458 for separation factor, and such predictions are further experimentally verified with a deviation much smaller than 1.0%.

References

Ali, M.B. and Hamrouni, B. (2016), "Development of a predictive model of the limiting current density of an electrodialysis process using response surface methodology", *Membr. Water Treat.*, **7**(2), 127-141.

Amirilargani, M. and Sadatnia, B. (2014), "Poly(vinyl alcohol)/zeolitic imidazolate frameworks (ZIF-8) mixed matrix membranes for pervaporation dehydration of isopropanol", *J. Membr. Sci.*, **469**, 1-10.

Amirilargani, M., Ghadimi, A., Tofighy, M.A. and Mohammadi, T. (2013), "Effects of poly(allylamine hydrochloride) as a new functionalization agent for preparation of poly vinyl alcohol/multiwalled carbon nanotubes membranes", *J. Membr. Sci.*, **447**, 315-324.

Amirilargani, M., Tofighy, M.A., Mohammadi, T. and Sadatnia, B. (2014), "Novel poly(vinyl alcohol)/multiwalled carbon nanotube nanocomposite membranes for pervaporation dehydration of isopropanol: Poly(sodium 4 styrenesulfonate) as a functionalization agent", *Ind. Eng. Chem. Res.*, **53**(32), 12819-12829.

Amnuaypanich, S., Patthana, J. and Phinyocheep, P. (2009), "Mixed matrix membranes prepared from natural rubber/poly(vinyl alcohol) semi-interpenetrating polymer network (NR/PVA semi-IPN) incorporating with zeolite 4A for the pervaporation dehydration of water-ethanol mixtures", *Chem. Eng. Sci.*, **64**(23), 4908- 4918.

Bolto, B., Hoang, M. and Xie, Z.L. (2011), "A review of membrane selection for the dehydration of aqueous ethanol by pervaporation", *Chem. Eng. Proc.*, **50**(3), 227-235.

Breck, D.W. (1964), *Zeolite Molecule Sieves*, John Wiley, New York, U.S.A.

Chew, S.C., Tan, C.P. and Nyam, K.L. (2017), "Application of response surface methodology for optimizing the deodorization parameters in chemical refining of kenaf seed oil", *Sep. Purif. Technol.*, **184**, 144-151.

Choudhari, S.K., Premakshi, H.G. and Kariduraganavar, M.Y. (2016), "Development of novel alginate-silica hybrid membranes for pervaporation dehydration of isopropanol", *Polym. Bull.*, **73**(3), 743-762.

Choudhury, S. and Ray, S.K. (2017), "Filled copolymer membranes for pervaporative dehydration of ethanol-water mixture", *Sep. Purif. Technol.*, **179**, 335-348.

Danmaliki, G.I., Saleh, T.A. and Shamsuddeen, A.A. (2017), "Response surface methodology optimization of adsorptive desulfurization on nickel/activated carbon", *Chem. Eng. J.*, **313**, 993-1003.

Das, P., Ray, S.K., Kuila, S.B., Samanta, H.S. and Singha, N.R. (2011), "Systematic choice of crosslinker and filler for pervaporation membrane: A case study with dehydration of isopropyl alcohol-water mixtures by polyvinyl alcohol membranes", *Sep. Purif. Technol.*, **81**(2), 159-173.

Deng, Y.H., Chen, J.T., Chang, C.H., Liao, K.S., Tung, K.L., Price, W.E., Yamauchi, Y. and Wu, K.C.W. (2016), "A drying-

free, water-based process for fabricating mixed-matrix membranes with outstanding pervaporation performance", *Angew. Chem. Int. Ed.*, **55**(41), 12793-12796.

Devi, V.K.P.J., Sai, P.S.T. and Balakrishnan, A.R. (2017), "Experimental studies and thermodynamic analysis of isobaric vapor-liquid-liquid equilibria of 2-propanol+water system using n-propyl acetate and isopropyl acetate as entrainers", *Flu. Phase Equilibr.*, **454**, 22-34.

Ding, C., Zhang, X.R., Li, C.C., Hao, X.G., Wang, Y.H. and Guan, G.Q. (2016), "ZIF-8 incorporated polyether block amide membrane for phenol permselective pervaporation with high efficiency", *Sep. Purif. Technol.*, **166**, 252-261.

Dogan, H. and Hilmioglu, N.D. (2010), "Zeolite-filled regenerated cellulose membranes for pervaporative dehydration of glycerol", *Vacuum*, **84**(9), 1123-1132.

Dudek, G., Gnus, M., Turczyn, R. and Konieczny, K. (2017), "The study of ethanol and water vapour permeation process through alginate membranes modified by magnetic powders", *Desalinat. Water Treat.*, **64**, 339-344.

Dudek, G., Gnus, M., Turczyn, R., Strzelewicz, A. and Krasowska, M. (2014), "Pervaporation with chitosan membranes containing iron oxide nanoparticles", *Sep. Purif. Technol.*, **133**, 8-15.

Dudek, G., Turczyn, R., Gnus, M. and Konieczny, K. (2018), "Pervaporative dehydration of ethanol/water mixture through hybrid alginate membranes with ferroferic oxide nanoparticles", *Sep. Purif. Technol.*, **193**, 398-407.

Fazlifard, S., Mohammadi, T. and Bakhtiari, O. (2017), "Chitosan/ZIF-8 mixed-matrix membranes for pervaporation dehydration of isopropanol", *Chem. Eng. Technol.*, **40**(4), 648-655.

Hua, D., Ong, Y.K., Wang, Y., Yang, T. and Chung, T.S. (2014), "ZIF-90/P84 mixed matrix membranes for pervaporation dehydration of isopropanol", *J. Membr. Sci.*, **453**, 155-167.

Huang, Z., Guan, H.M., Tan, W.L., Qiao, X.Y. and Kulprathipanja, S. (2006a), "Pervaporation study of aqueous ethanol solution through zeolite-incorporated multilayer poly(vinyl alcohol) membranes: Effect of zeolites", *J. Membr. Sci.*, **276**(1-2), 260-271.

Huang, Z., Shi, Y., Wen, R., Guo, Y.H., Su, J.F. and Matsuura, T. (2006b), "Multilayer poly(vinyl alcohol)-zeolite 4A composite membranes for ethanol dehydration by means of pervaporation", *Sep. Purif. Technol.*, **51**(2), 126-136.

Jia, Z.Q. and Wu, G.R. (2016), "Metal-organic frameworks based mixed matrix membranes for pervaporation", *Micropor. Mesopor. Mater.*, **235**, 151-159.

Jiang, L.Y., Chung, T.S. and Rajagopalan, R. (2007), "Matrimid (R)/MgO mixed matrix membranes for pervaporation", *AIChE J.*, **53**(7), 1745-1757.

Kang, C.H., Lin, Y.F., Huang, Y.S., Tung, K.L., Chang, K.S., Chen, J.T., Hung, W.S., Lee, K.R. and Lai, J.Y. (2013), "Synthesis of ZIF-7/chitosan mixed-matrix membranes with improved separation performance of water/ethanol mixtures", *J. Membr. Sci.*, **438**, 105-111.

Khoonsap, S. and Amnuaypanich, S. (2011), "Mixed matrix membranes prepared from poly(vinyl alcohol) (PVA) incorporated with zeolite 4A-graft-poly(2-hydroxyethyl methacrylate) (zeolite-g-PHEMA) for the pervaporation dehydration of water–acetone mixtures", *J. Membr. Sci.*, **367**(1-2), 182-189.

Khosravi, T., Mosleh, S., Bakhtiari, O. and Mohammadi, T. (2012), "Mixed matrix membranes of Matrimid 5218 loaded with zeolite 4A for pervaporation separation of water-isopropanol mixtures", *Chem. Eng. Res. Des.*, **90**(12), 2353-2363.

Mahdi, T., Ahmad, A., Nasef, M.M. and Ripin, A. (2015), "State-of-the-art technologies for separation of azeotropic mixtures", *Sep. Purif. Rev.*, **44**(4), 308-330.

Malekpour, A., Mostajeran, B. and Koohmareh, G.A. (2017), "Pervaporation dehydration of binary and ternary mixtures of acetone, isopropanol and water using polyvinyl alcohol/zeolite membranes", *Chem. Eng. Proc.*, **118**, 47-53.

Mosleh, S., Khosravi, T., Bakhtiari, O. and Mohammadi, T. (2012), "Zeolite filled polyimide membranes for dehydration of isopropanol through pervaporation process", *Chem. Eng. Res. Des.*, **90**(3), 433-441.

Olukman, M. and Sanli, O. (2015), "A novel in situ synthesized magnetite containing acrylonitrile and 2-hydroxyethyl methacrylate grafted poly(vinyl alcohol) nanocomposite membranes for pervaporation separation of acetone/water mixtures", *Chem. Eng. Proc.*, **98**, 60-70.

Ong, Y.K., Shi, G.M., Le, N.L., Tang, Y.P., Zuo, J., Nunes, S.P. and Chung, T.S. (2016), "Recent membrane development for pervaporation processes", *Prog. Polym. Sci.*, **57**, 1-31.

Premakshi, H.G., Ramesh, K. and Kariduraganavar, M.Y. (2015), "Modification of crosslinked chitosan membrane using NaY zeolite for pervaporation separation of water-isopropanol mixtures", *Chem. Eng. Res. Des.*, **94**, 32-43.

Razavi, S., Sabetghadam, A. and Mohammadi, T. (2011), "Dehydration of isopropanol by PVA-APTEOS/TEOS nanocomposite membranes", *Chem. Eng. Res. Des.*, **89**(2), 148-155.

Sajjan, A.M., Kumar, B.K.J., Kittur, A.A. and Kariduraganavar, M.Y. (2013), "Novel approach for the development of pervaporation membranes using sodium alginate and chitosan-wrapped multiwalled carbon nanotubes for the dehydration of isopropanol", *J. Membr. Sci.*, **425**, 77-88.

Salehian, P. and Chung, T.S. (2017a), "Two-dimensional (2D) particle coating on membranes for pervaporation dehydration of isopropanol: A new approach to seal defects and enhance separation performance", *J. Membr. Sci.*, **544**, 378-387.

Salehian, P. and Chung, T.S. (2017b), "Thermally treated ammonia functionalized graphene oxide/polyimide membranes for pervaporation dehydration of isopropanol", *J. Membr. Sci.*, **528**, 231-242.

Shi, G.M., Yang, T.X. and Chung, T.S. (2012), "Polybenzimidazole (PBI)/zeolitic imidazolate frameworks (ZIF-8) mixed matrix membranes for pervaporation dehydration of alcohols", *J. Membr. Sci.*, **415**, 577-586.

Shirazi, Y., Tofighy, M.A. and Mohammadi, T. (2011), "Synthesis and characterization of carbon nanotubes/poly vinyl alcohol nanocomposite membranes for dehydration of isopropanol", *J. Membr. Sci.*, **378**(1-2), 551-561.

Smitha, B., Suhanya, D., Sridhar, S. and Ramakrishna, M. (2004), "Separation of organic-organic mixtures by pervaporation-a review", *J. Membr. Sci.*, **241**(1), 1-21.

Vural, N., Cavuldak, O.A. and Anli, R.E. (2018), "Multi response optimisation of polyphenol extraction conditions from grape seeds by using ultrasound assisted extraction (UAE)", *Sep. Sci. Technol.*, **53**(10), 1540-1551.

Wang, N.X., Zhang, G.J., Wang, L., Li, J., An, Q.F. and Ji, S.L. (2017), "Pervaporation dehydration of acetic acid using NH_2-UiO-66/PEI mixed matrix membranes", *Sep. Purif. Technol.*, **186**, 20-27.

Wang, Q.Z., Li, N., Bolto, B., Hoang, M. and Xie, Z.L. (2016), "Desalination by pervaporation: A review", *Desalinat.*, **387**, 46-60.

Wang, X.L., Chen, J.X., Fang, M.Q., Wang, T., Yu, L.X. and Li, J.D. (2016), "ZIF-7/PDMS mixed matrix membranes for pervaporation recovery of butanol from aqueous solution", *Sep. Purif. Technol.*, **163**, 39-47.

Wang, Y., Goh, S.H., Chung, T.S. and Na, P. (2009), "Polyamide-imide/polyetherimide dual-layer hollow fiber membranes for pervaporation dehydration of C1-C4 alcohols", *J. Membr. Sci.*,

326(1), 222-233.
Zafar, M., Ali, M., Khan, S.M., Jamil, T. and Butt, M.T.Z. (2012), "Effect of additives on the properties and performance of cellulose acetate derivative membranes in the separation of isopropanol/water mixtures", *Desalinat*., **285**, 359-365.
Zhang, Z.G., Zhang, L., Zhang, Q.Q., Sun, D.Z., Pan, F.J., Dai, S.W. and Li, W.X. (2016), "Separation of 2-propanol and water azeotropic system using ionic liquids as entrainers", *Flu*. *Phase Equilibr*., **412**, 94-100.

CC